Exchange-bias training effect in TbFe/ GdFe: Micromagnetic mechanism

Thomas Hauet, S Mangin, J Mccord, F Montaigne, Eric E. Fullerton

Exchange-bias training effect in TbFe/GdFe: Micromagnetic mechanism

T. Hauet,[1] S. Mangin,[1] J. McCord,[2] F. Montaigne,[1] and Eric E. Fullerton[3]
[1]*Laboratoire de Physique des Matériaux, Nancy-Université, CNRS, Boîte Postal 239, F-54506 Vandœuvre les Nancy, France*
[2]*Leibniz Institute for Solid State and Materials Research IFW Dresden, Institute for Metallic Materials, Postfach 270116, D-01171 Dresden, Germany*
[3]*Center for Magnetic Recording Research, University of California San Diego, La Jolla, California 92093-0401, USA*
(Received 2 March 2007; revised manuscript received 3 September 2007; published 18 October 2007)

We present magnetization and Kerr microscopy measurements of the exchange-bias training effect in hard/soft, $Tb_{12}Fe_{88}/Gd_{40}Fe_{60}$, bilayers. These experimental results, compared with micromagnetic simulations, unambiguously show the role of the soft GdFe layer reversal on irreversible magnetic changes in the hard TbFe layer. After a partial reversal of the GdFe magnetization layer, the next field cycle exhibits a double hysteresis loop which is due to the existence of two types of domains in the sample, and only one of these domains has been subject to the training effect. The antiferromagnetically interfacial coupling and positive exchange-bias shift permit us to exclude any direct contribution from the magnetic field to this mechanism.

DOI: 10.1103/PhysRevB.76.144423 PACS number(s): 75.30.Et, 75.60.Jk, 75.70.Cn

Exchange-bias phenomena have been extensively studied for antiferromagnetic (AF) and ferromagnetic (FM) bilayer systems over the past twenty years.[1,2] Exchange biased systems are typically set by cooling the AF/FM bilayers through the blocking temperature of the AF layers, under a cooling field H_{CF}. The resulting hysteresis loop of the FM layer is shifted from the origin by the exchange bias field H_E. The same phenomena have been observed in other exchange-coupled bilayers using ferromagnetic and ferrimagnetic materials.[1,3] It has also been demonstrated that for bilayer structures exhibiting an antiferromagnetic interface exchange coupling both positive and negative H_E values can be obtained.[3,4] Recently, interest is growing on understanding training of the exchange bias effect, where the value of H_E evolves with consecutive hysteresis loops.[5] A decrease of H_E toward 0 with the number of cycles has been observed for the ferromagnetically exchange coupled samples,[6,7] whereas, for antiferromagnetically exchange coupled bilayers, a variation from a negative to a positive H_E value has been measured as the field is cycled.[8] It is generally believed that a nonstationary exchange bias indicates the rearrangement of the spin structure mediating the interaction between the AF and FM toward equilibrium.[5,9] Below the blocking temperature, the magnetic configuration is trapped in a metastable configuration, and through cycling, it then evolves to a more stable state. However, a detailed understanding of the mechanisms leading to training effect in the AF/FM bilayer is lacking because one has to consider metastable configurations in the AF layer which are difficult to simulate and to observe experimentally.

Insight into the training effect has been gained by studying hard/soft ferromagnetic[10] and ferrimagnetic/ferrimagnetic[8] bilayers. The latter consists of antiferromagnetically coupled $Tb_{12}Fe_{88}/Gd_{40}Fe_{60}$ bilayers. For both alloys the moment held by the rare-earth is antiparallel to the Fe spin. The magnetization of the GdFe layer is parallel to the Gd moments, whereas the TbFe magnetization is parallel to the Fe spin. Because the exchange coupling is dominated by the Fe-Fe ferromagnetic interaction an antiferromagnetic coupling is present at the interface between the two alloys' net magnetizations. GdFe is a soft material for all temperature with a growth-induced in-plane uniaxial anisotropy. TbFe is a soft magnetic material at room temperature but hardens with the development of a strong random anisotropy at reduced temperature and exhibits coercive fields larger than 10^4 Oe at low temperature. The magnetic response of the TbFe/GdFe bilayer at low temperatures is similar to the exchange bias field behavior of FeF_2/Fe,[3,4] i.e. a transition from negative to positive H_E as H_{CF} increases. This behavior in TbFe/GdFe bilayers was shown to result from an interfacial domain wall (IDW) that forms at the TbFe/GdFe interface and is frozen into the TbFe when the sample is cooled. Previous magnetization and magnetoresitive measurements, compared with a one-dimensional spin chain model, proved that the shape of this IDW and more precisely the orientation of the TbFe magnetization at the interface depends on the magnitude of the cooling field and determines H_E. Polarized neutron reflectometry (PNR) measurements indicated that the frozen IDW is metastable and that the exchange bias training effect in TbFe/GdFe results from the relaxation of the IDW with field cycling.

In spite of the understanding of the training effect's origin, the relaxation mechanism during field cycling is not clear. Our previous results on hard/soft TbFe/GdFe bilayers suggest that the evolutions of magnetic configurations in the hard layer are strongly correlated with the reversal of the soft layer.[8] However, the relaxation process has also been thought to be exclusively dependent on the deviation of the hard (or AF) interface magnetization from its equilibrium value, i.e., independent from microscopic details of the magnetization reversal of the soft (or FM) layer.[9] Moreover, a direct interaction between the magnetic field and the hard layer magnetization has also been proposed.[11]

In the present paper, we focus on the role of the GdFe magnetization reversal mechanism on the training in the TbFe layer. Magnetization measurements combined with Kerr microscopy allow us to follow the magnetic configuration of both the soft and the hard layer during minor loops. A direct correlation of the GdFe reversal on the irreversible changes in the TbFe is found, whereas no direct influence of the field is observed. In addition we demonstrate the impor-

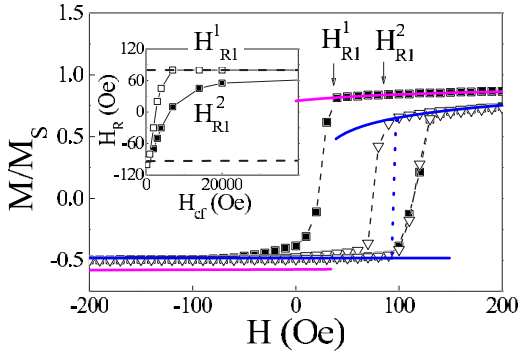

FIG. 1. (Color online) Normalized magnetization as a function of the field applied along the easy axis for the GdFe/TbFe bilayer at 15 K after cooling from 300 K in H_{CF}=7 kOe. Two successive hysteresis loops are shown (full symbols correspond to the first one and open symbols to the second one). The lines correspond to the results of a micromagnetic calculation considering the sample as a 1D spin chain in which the TbFe configuration is frozen. The pink solid lines correspond to the case where the angle between the fixed interfacial TbFe spin and the positive field is θ_i^{TbFe}=70°. The blue solid lines correspond to θ_i^{TbFe}=0°. The dashed blue line corresponds to the field where the energies of positive magnetization and negative magnetization states are equal. The inset shows the evolution of the reversal field during the descending branch for the first $H^1{}_{R1}$ and the second hysteresis loop ($H^2{}_{R1}$) as a function of the cooling field value.

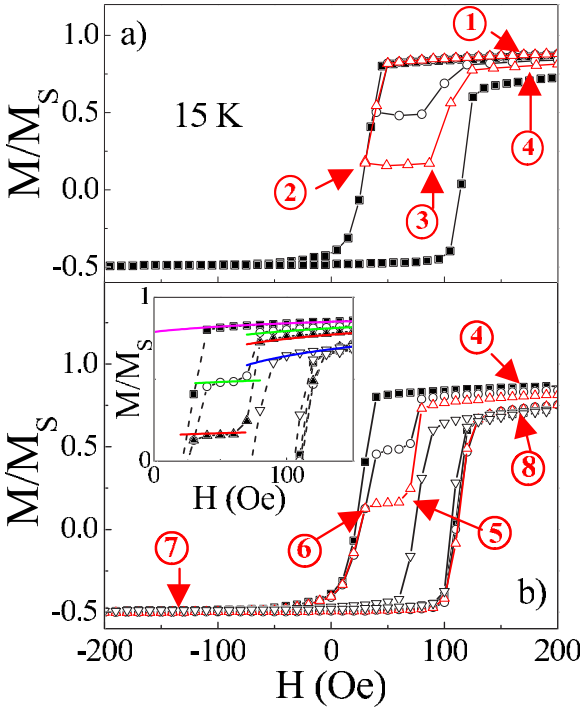

FIG. 2. (Color online) (a) Minor loop cycles performed after cooling the glass/TbFe/GdFe/Al sample from 300 to 15 K under 7 kOe. Square symbols represent the +200 Oe→−200 Oe→+200 Oe hysteresis cycle. Open circles, resp. open triangles, correspond to minor cycles with H_X=40 Oe, respectively, H_X=30 Oe. (b) Second hysteresis cycles measured at 15 K after cooling the sample under 7 kOe from 300 K and doing a first minor cycle from 200 Oe down to H_X=200 (full squares), 40 (open circles), 30 (open triangles), and −200 Oe (crosses). The lines correspond to the results of a micromagnetic calculation considering the sample as the sum of two independent 1D spin chains characterized by a frozen TbFe configuration with θ_i^{TbFe}=0° and 70°, respectively. The sample magnetization was calculated as the sum of the magnetizations resulting from both spin chains taking into account the area occupied by each chain. The pink line corresponds to the case where the θ_i^{TbFe}=0° chain area is null. The green, red, and blue lines are the calculated magnetization considering, respectively, a covering ratio of 26, 50, and 100% for the θ_i^{TbFe}=0° chain.

tance of lateral domain motion on the in-plane interfacial domain wall evolution.

The results shown in Figs. 1–3 were obtained on a glass/$Tb_{12}Fe_{88}$ (50 nm)/$Gd_{40}Fe_{60}$ (100 nm)/Al (5 nm) sample. This ferrimagnetic/ferrimagnetic amorphous bilayer was grown by coevaporation on substrate kept at liquid nitrogen temperature. Atomic force microscopy measurements showed a typical 0.5-nm roughness. Magnetic measurements were performed with a commercial superconducting quantum interference device (SQUID) magnetometer. Figure 1 displays two consecutive hysteresis loops (+200 Oe→−200 Oe→+200 Oe) obtained after cooling the sample from 300 to 15 K under a cooling field H_{CF}=7 kOe. A pronounced training effect is clearly evidenced by the reduction of the coercive fields and the shift of the loop center comparing the first and second hysteresis loops. However, rather than considering the exchange bias and the coercive fields, it is more relevant to discuss the reversal fields $H^1{}_{R1}$ ($H^2{}_{R1}$) and $H^1{}_{R2}$ ($H^2{}_{R2}$) for the descending and ascending branch of the first (second) minor loop, respectively. Indeed, in Fig. 1, the evolution of the exchange bias field results only from a change between the descending branch reversals $H^1{}_{R1}$ and $H^2{}_{R1}$ values. Comparing $H^1{}_{R2}$ and $H^2{}_{R2}$ no change is observed. These observations are in agreement with the assumption that most of the training effect acts during the initial descending branch and not during the ascending branch. Moreover, the training effect is found to depend on the cooling field H_{CF} amplitude as suggested by the evolution of $H^1{}_{R1}$ and $H^1{}_{R2}$, shown in the inset of Fig. 1. For low cooling fields, little or no training effect is observed. As H_{CF} increases, H_E shifts toward positive fields and the difference between $H^1{}_{R1}$ and $H^1{}_{R2}$ increases as well until $H^1{}_{R2}$ reaches its maximum value.

The evolution of the TbFe/GdFe magnetic configuration at 15 K can be calculated considering a one-dimensional micromagnetic calculation which has already been used successfully in the past.[22,3,12] For this calculation the TbFe magnetization is assumed fixed for all applied fields. As a consequence only θ_i^{TbFe}, the angle between the frozen TbFe spins at the interface and the positive field direction, is taken into account. The GdFe layer is treated as a spin chain (200 spins) perpendicular to the TbFe/GdFe interface. To obtain the possible metastable magnetic configurations, the total magnetic energy is minimized taking into account exchange interaction between neighbor spins, uniaxial magnetocrystalline anisotropy, and the Zeeman interaction.[22] The parameters used are the saturation magnetization M =1000 emu/cm^3, the anisotropy constant K=10^5 erg/cm^3,

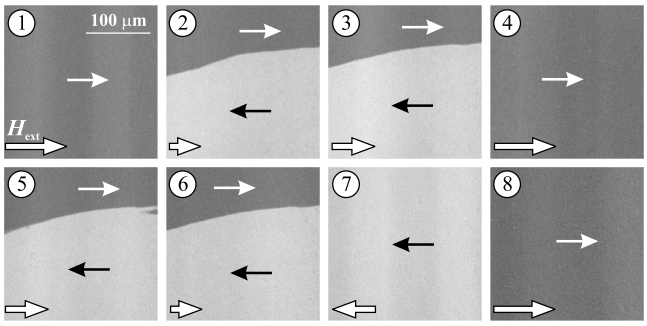

FIG. 3. Magnetic domain configurations of glass/TbFe/GdFe/Al sample for fields 1–8 indicated in Fig. 2. The magnetic field directions and amplitudes corresponding to Fig. 2 are indicated at the left bottom of each picture. The magnetization directions in the GdFe layer are sketched.

and the bulk exchange stiffness $A=6.10^{-7}$ erg/cm of GdFe at 15 K, as well as exchange coupling across the GdFe/TbFe interface $J=-7$ erg/cm^2 known from previous studies.[3,12,22] In Fig. 1, for the first descending magnetization branch ($+200$ Oe$\rightarrow H^1_{R1}\approx 20$ Oe) measured after cooling the sample under $H_{CF}=7$ kOe a good agreement is obtained by assuming $\theta_i^{\mathrm{TbFe}}=70°$. This is consistent with previous polarized neutron reflectometry measurements performed at 15 K, for $H_{CF}=7$ kOe, which concluded an interface TbFe magnetization orientation such that $\theta_i^{\mathrm{TbFe}}=70°$.[8] As the TbFe magnetization is assumed fixed, the GdFe magnetization then adopts the magnetic configuration, which minimizes the interface exchange coupling and the Zeeman energy terms. This results in a partial IDW in the GdFe. In Fig. 1, the micromagnetic simulation fits the first descending branch very well before H^1_{R1}. After the reversal at H^1_{R1} the magnetization curve is no longer properly fitted by the calculation assuming $\theta_i^{\mathrm{TbFe}}=70°$. The best fit is then obtained for $\theta_i^{\mathrm{TbFe}}=0°$ (Fig. 1). In that case, the GdFe is uniformly magnetized with its magnetization pointing toward negative field direction. This GdFe state is kept as the field is swept back from -200 Oe to positive field until $H^1_{R2}\approx +100$ Oe. For this field, GdFe magnetization reverses and a 180° domain wall is created in the GdFe depth to satisfy the antiferromagnetic coupling at the interface; its evolution as a function of the field calculated with our 1D simulation is in good agreement with the experimental data (Fig. 1). We note that the use of $\theta_i^{\mathrm{TbFe}}=0°$ in the simulation is fully coherent with the uniform TbFe magnetization found at -200 Oe during our previous PNR measurements.[8] Moreover, if the calculated exchange bias field is defined as the field for which the energy of the two GdFe states are equal[12] then the calculated and measured exchange bias field are identical, $H^2_E=90$ Oe (Fig. 1). Finally, in addition to the evolution of the exchange bias values, the changes of M_{shift}, shift in magnetization of the hysteresis biased loops which is directly related to the frozen TbFe magnetization, observed in Fig. 1 confirms this TbFe relaxation.[3,21]

To gain a deeper understanding of the reorientation mechanism leading to the TbFe spins structure, we measured "minor" loop hysteresis curves ($+200$ Oe$\rightarrow H_X\rightarrow +200$ Oe), followed by a "regular" loop measurement ($+200$ Oe$\rightarrow -200$ Oe$\rightarrow +200$ Oe). In the case $H_X>H^1_{R1}$ the minor loop has no effect on the subsequent $M(H)$ loops. Conversely, for $H_X<-100$ Oe hysteresis loops comparable to the ones shown in Fig. 1 are measured. Figure 2(a) represents the hysteresis cycles performed at 15 K for $H_X=40$, 30, and -200 Oe. For the two first cases, only part of the GdFe magnetization reverses before the field is swept back to $+200$ Oe. As a second hysteresis loop is successively measured, two jumps are observed in the descending branch. The first jump occurs at a field close to H^2_{R1} whereas the second jump occurs for H^1_{R1}. Note that the amplitude of the jumps at H^2_{R1} [Fig. 2(a)] are equal to the jump occurring in the "minor" loop [Fig. 2(b)]. The same behavior was observed for six cooling field values between 200 Oe and 10 kOe. This indicates that the same mechanism or excitation governs the exchange bias training effect phenomenon, independently of the amplitude changes.

To identify the origin of this double loop, we imaged the lateral magnetic domain structure by magneto-optical Kerr microscopy under varying magnetic fields in an optical cryostat.[13,14] With the sample mentioned above, only the GdFe layer is probed, because its thickness (50 nm) exceeds the penetration depth of light. Figure 3 represents images corresponding to the different fields as marked in Figs. 2(a) and 2(b). At 200 Oe [Fig. 3(1)] the GdFe magnetization is aligned with the positive field direction. Our previous PNR measurements showed that the GdFe magnetization was not uniform but that a partial IDW was present at the interface. Because this IDW is small compared with the total GdFe layer thickness and is located at the interface of the bilayer, it has not been observed. The image taken at H_X close to H^1_{R1} shows that the sample magnetization is split into domains with nearly antiparallel orientation of magnetization [Fig. 3(2)]. Those domains are separated by a domain wall, designated as the lateral domain wall (LDW) to be differentiated from the interface domain wall (IDW). This explains how an intermediate magnetization value may be reached. The GdFe magnetization reversal is dominated by lateral domain wall motion. As the field is swept back along the easy axis, in accordance with the hysteresis measurements the domain structure is maintained [Fig. 3(3)]. At $H=H^1_{R2}$, the LDW propagates back and the domain structure is annihilated. For $H=200$ Oe [Fig. 3(4)], the GdFe magnetization is in the positive field direction and appears identical to Fig. 3(1). As the second loop is performed, again, LDW propagation is observed. However, when the field decreases from 200 Oe to a value below H^2_{R1}, the GdFe magnetization starts to switch and the same domain configuration as seen in Fig. 3(3) reappears [Fig. 3(5)]. This state is unchanged until $H=H_X$ [Fig. 3(6)]. For lower fields the GdFe magnetization is completely reversed [Fig. 3(7)].

These observations demonstrate that the partial reversing of the GdFe layer magnetization, during the first minor loop, generates a coexistence of two types of "bilayer domains." Indeed, comparison between Figs. 3(3) and 3(5) indicates that the part of the sample, which has been submitted to GdFe reversal, switches at H_{R2}. The Kerr images elucidate the bifurcated loop [Fig. 2(b)]. After the first cycle, each domain gives rise to its own independent exchange bias field.

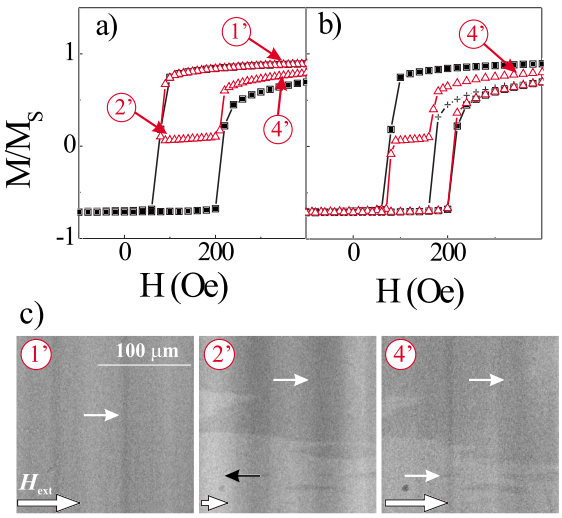

FIG. 4. (Color online) (a) Major (full square) and a minor (open triangle) loops performed after cooling the sample B from 300 to 15 K under 7 kOe. (b) Second hysteresis cycles measured at 15 K after the major (cross) and the minor (open triangle) presented in (a). (c) Kerr microscopy images visualized on sample B corresponding to the state 1′, 2′, and 4′ defined on (a) and (b). The proposed magnetization directions in the hidden GdFe layer are indicated.

Such double loop behavior has also been observed in AF/FM bilayers after the systems had been cooled down in a multidomain state[15–17] and for hard/soft ferrimagnetic TbFe/GdFe bilayers.[18] We used an extension of the one-dimensionnal micromagnetic simulation presented above to confirm the above conclusions. The sample is considered to be made of two magnetically independent 1D spin chains containing, respectively, the TbFe state before ($\theta_i^{\mathrm{TbFe}}=70°$) and after ($\theta_i^{\mathrm{TbFe}}=0°$) relaxation. The sample magnetization was calculated as the sum of the magnetizations resulting from both spin chains taking into account the area occupied by each chain. On the all range of field from 200 Oe to −200 Oe, a good agreement between theoretical magnetic curves and experimental data was obtained as shown in inset of Fig. 2(b). For the case of $H_X=40$ Oe, the magnetization variations are well reproduced considering that 26% of the sample area is covered by the relaxed spin chain, while the two chains have been considered to have the same area for $H_X=30$ Oe. Note that no quantitative correlation between magnetization curves and Kerr microscopy is possible since the Kerr images are showing only a small part of the sample used for SQUID measurements.

To directly image the irreversible changes in the TbFe layer during the GdFe reversal, we performed Kerr microscopy on a second sample, glass$\|$$Gd_{40}Fe_{60}$ (50 nm)/$Tb_{12}Fe_{88}$ (15 nm)/Al (5 nm), with the TbFe layer on top. We reproduced the magnetization procedure and Kerr microscopy measurements on this second sample. After cooling the bilayer in a field of 7 kOe down to 15 K, the different minor and major hysteresis loops shape, measured on this second sample, were very similar to the ones measured on GdFe on the other sample [Figs. 4(a) and 4(b)]. The enhancement of H_{R1} values ($H^1_{R1}=80$ Oe and $H^2_{R1}=220$ Oe) is due to the thickness differences between the samples and does not affect the training processes. We observe essentially the same features as on the first bilayer sample for all tested values of H_{CF}. In Fig. 4(c), we present the TbFe magnetic domain structure visualized for the states 1′, 2′, 4′ equivalent to the states 1, 2, 4 noted in Fig. 2(a), during the first minor loop. Immediately after cooling the sample, for $H>H^1_{R1}$, a laterally uniform configuration is imaged. This configuration changes as the GdFe starts to reverse. A different domain structure appears at $H=H_X$ as the GdFe magnetization is partially switched [Fig. 4 (2′)]. Two types of domain are visible. Whereas one is identical to the original state, the second domain presents a different averaged magnetization. Moreover, as the field is increased again to 350 Oe, the magnetization in the GdFe layer reverses back (Fig. 2), yet the lateral domain pattern persists [Fig. 4 (4′)], but a reduction of the domain contrast is observed [Figs. 4 (2′) and 4 (4′)]. These observations prove that irreversible changes occur in the TbFe as a result of the GdFe reversal. The decrease in magneto-optical domain contrast, comparing the images in Figs. 4 (2′) and 4 (4′)], indicates that the observed changes in magnetization come mainly from the GdFe reversal imaged through the TbFe layer. The fact that the new domain structure remains after reversing the GdFe magnetization in the positive field direction agrees with an irreversible relaxation of one lateral part of the TbFe layer at the interface in a more stable state. Figure 4(c) provides direct evidence that, in the hard/soft $Tb_{12}Fe_{88}/Gd_{40}Fe_{60}$ bilayer, the relaxation of the TbFe frozen IDW relaxation, which governs training effect phenomenon, is directly induced by the GdFe reversal. This process appears to act similarly to a torque generated by the FM magnetization on AF spins in AF/FM bilayers, which then induces irreversible changes in the AF layer.[19,20] Indeed, in both cases, changes in the hard (or AF) layer is made possible because of multiple stable and metastable magnetic configurations available to the hard layer. For the current system the most stable one corresponds to a TbFe layer uniformly magnetized pointing in the positive field direction. When the GdFe magnetization reverses in the negative field direction, the antiferromagnetic coupling at the interface tends to reorient the TbFe in the positive field direction. So the GdFe magnetization reversal allows the system to reach a more stable configuration.[5] Finally, as a result of the positive exchange bias field case, a specificity of these experiments, the applied field was always kept positive during the minor loops. Hence we can conclude that the exchange bias training is activated by the soft layer magnetization reversal and the applied field reversal, itself, has no direct role on the training effect stimulation.

In conclusion, we used an antiferromagnetically exchange coupled hard/soft system, $Tb_{12}Fe_{88}/Gd_{40}Fe_{60}$, to study the mechanism allowing the relaxation of the frustrated hard layer, i.e., exchange bias training effect. Magnetization measurements combined with Kerr microscopy permitted to the follow the magnetic configuration in both GdFe and TbFe layers during field cycling. We observe that a partial reversal of the GdFe magnetization by lateral domain wall (LDW) propagation generates new TbFe magnetic domains, which

have been subjected to a training effect. Our experiments evidenced that the training effect is due to an irreversible reorientation of the hard layer magnetization . This reorientation process depends on microscopic details of the magnetization reversals of the soft GdFe layer, whereas the applied field is proved to have no direct effect on the relaxation of the hard TbFe layer.

We thank D. Ligiardi, D. Pierre, F. Mouginet, and M. Alnot for help with experiments.

[1] J. Nogues and I. K. Schuller, J. Magn. Magn. Mater. **192**, 203 (1999), and references therein.
[2] R. L. Stamps, J. Phys. D **33**, R247 (2000).
[3] S. Mangin, F. Montaigne, and A. Schuhl, Phys. Rev. B **68**, 140404(R) (2003).
[4] J. Nogues, D. Lederman, T. J. Moran, and I. K. Schuller, Phys. Rev. Lett. **76**, 4624 (1996); J. Nogues, C. Leighton, and I. K. Schuller, Phys. Rev. B **61**, 1315 (2000).
[5] A. Hoffmann, Phys. Rev. Lett. **93**, 097203 (2004).
[6] A. Hochstrat, C. Binek, and W. Kleemann, Phys. Rev. B **66**, 092409 (2002).
[7] J. Keller, P. Miltényi, B. Beschoten, G. Güntherodt, U. Nowak, and K. D. Usadel, Phys. Rev. B **66**, 014431 (2002); *ibid.* **66**, 014431 (2002).
[8] T. Hauet, J. A. Borchers, Ph. Mangin, Y. Henry, and S. Mangin, Phys. Rev. Lett. **96**, 067207 (2006).
[9] C. Binek, Phys. Rev. B **70**, 014421 (2004).
[10] C. Binek, S. Polisetty, X. He, and A. Berger, Phys. Rev. Lett. **96**, 067201 (2006).
[11] R. K. Zheng, G. H. Wen, K. K. Fung, and X. X. Zhang, Phys. Rev. B **69**, 214431 (2004).
[12] Y. Henry, S. Mangin, T. Hauet, and F. Montaigne, Phys. Rev. B **73**, 134420 (2006).
[13] Actually our model predicts the exchange bias field H_E which is close to H^1_{R1} considering the low coercive field of our system. See Ref. 12 for more details.
[14] O. de Haas, R. Schäfer, L. Schultz, C. M. Schneider, Y. M. Chang, and M. T. Lin, Phys. Rev. B **67**, 054405 (2003).
[15] O. Petracic, Zhi-Pan Li, Igor V. Roshchin, M. Viret, R. Morales, X. Batlle, and I. K. Schuller, Appl. Phys. Lett. **87**, 222509 (2005).
[16] C. L. Chien, V. S. Gornakov, V. I. Nikitenko, A. J. Shapiro, and R. D. Shull, Phys. Rev. B **68**, 014418 (2003).
[17] S. Bruck, J. Sort, V. Baltz, S. Surinach, J. S. Munoz, B. Dieny, M. D. Baro, and J. Nogues, Adv. Mater. (Weinheim, Ger.) **17**, 29281 (2005).
[18] S. Mangin, T. Hauet, Y. Henry, F. Montaigne, and E. E. Fullerton, Phys. Rev. B **74**, 024414 (2006).
[19] J. McCord, R. Mattheis, and D. Elefant, Phys. Rev. B **70**, 094420 (2004).
[20] L. Wee, R. L. Stamps, L. Malkinski, and Z. Celinski, Phys. Rev. B **69**, 134426 (2004).
[21] J. Sort, A. Popa, B. Rodmacq, and B. Dieny, Phys. Rev. B **70**, 174431 (2004).
[22] F. Montaigne, S. Mangin, and Y. Henry, Phys. Rev. B **67**, 144412 (2003).